Phase Separation Dynamics of Aqueous Poly [(2-ethoxy) ethoxy ethyl vinyl ether] Solutions as Explored using the Laser T-Jump Technique Combined With Photometry

Yasuyuki Tsuboi,* Kanae Kikuchi, Noboru Kitamura, Hiroaki Shimomoto, Shokyoku Kanaoka, Sadahito Aoshima

Poly[(2-ethoxy) ethoxy ethyl vinyl ether] (poly(EOEOVE)) is a representative thermoresponsive polymer in aqueous solution for which the time constants of the phase separation (PS) are determined with high accuracy. It is revealed that the PS dynamics of the polymer are entirely different from those of the poly(*N*-isopropylacrylamide) (PNIPAM) system, which is an alternative representative thermoresponsive polymer. Poly(EOEOVE) exhibits complicated PS behavior that is described using double exponential functions. The PS of poly(EOEOVE) is much faster than the PS of PNIPAM in aqueous solutions and becomes faster with increasing concentration of the polymer. PS behavior that is particular to the present system is successfully understood within the framework of the aggregation mechanism.

1. Introduction

Since the first discovery of the phenomenon, thermoresponsive polymers have attracted much attention in various research fields.[1–3] A representative specimen is poly(*N*-isopropylacrylamide) (PNIPAM), which contains both hydrophilic and hydrophobic functional groups in the structure. At room temperature, the polymer dissolves homogeneously in water, adopting a random coiled structure. Upon temperature elevation above the lower critical solution temperature (LCST), it turns into a globular structure accompanied by dehydration of the polymer chains, followed by molecular aggregation due to hydrophobic interactions among the globules. As a result, the solution exhibits macroscopic phase separation (PS) into water-rich and polymer-rich phases. This behavior is of great interest, involving a wealth of science such as the volume exclusion theory, polymer kinetics and dynamics, and polymer solution theories.[4] Moreover, as a matter of course, such thermoresponsive phenomena have potential applications toward various functional materials such as drug-delivery systems because the LCST of PNIPAM is close to human body temperature.[5]

So far, much effort has been expended in efforts to understand the fundamental mechanism underlying these phenomena and to reveal an overview of the phenomena. It should be pointed out that a large proportion of the past studies have concentrated on static characteristics involving the structures, solute–solvation interactions, and the energy levels of the polymers. Indeed, the

Y. Tsuboi, K. Kikuchi, N. Kitamura
Division of Chemistry, Graduate School of Science,
Hokkaido University, Sapporo 060-0810, Japan
E-mail: twoboys@sci.hokudai.ac.jp
Y. Tsuboi
Japan Science and Technology Corporation (JST),
PRESTO, Yobancho 5-3, Chiyoda-ku 102-8666, Tokyo, Japan
H. Shimomoto, S. Kanaoka, S. Aoshima
Division of Macromolecular Science,
Graduate School of Science, Osaka University,
Toyonaka 565-0043, Osaka, Japan

DOI: 10.1002/macp.201100540

synthesis of numerous polymers such as these,[6] structural analyses using various spectroscopic and light-scattering methodologies,[7–13] thermodynamic analyses (i.e., differential scanning calorimery (DSC)),[14,15] and theoretical as well as experimental approaches[16] to draw precise phase diagrams have been performed on these polymers over the past decades.

By contrast, little is known about the dynamics of thermoresponsive PS, or of associated phase transitions. It should be noted that the dynamics of volume phase transitions in thermoresponsive gels (i.e., cross-linked PNIPAM) in water have been revealed, both by experimental and theoretical methods.[17–20] However, in the case of solution systems (not cross-linked polymers) that show a LCST or UCST (upper critical solution temperature), even fundamental information such as the time-scale of PS, their structures, their molecular weights ($\overline{M}_w$) and the concentration dependence of their PS dynamics still remain unclear. To completely understand the real picture of PS in such polymer systems, it is indispensable to clarify the dynamic behavior of PS and to adequately correlate it with the static properties of sample polymers.

So far, several research groups have developed their original experimental technique and applied those to approach kinetics and dynamic behavior of coil-globule transition as well as PS/mixing (demixing and remixing). In particular, Van Mele and co-workers have systematically revealed demixing/remixing kinetics for several thermoresponsive polymers by means of modulated temperature DSC.[15,21–24] The obtained new insights into it are as follows: (1) remixing is slower than demixing, (2) vitrification of a polymer rich phase slows down demixing, (3) demixing and remixing takes place within 100 s, followed by slow (several hundred of minutes) relaxation, and (5) the rate of demixing/remixing is sensitive of chemical structure of sample polymer. In addition to these researches, Sun et al.[25,26] have explored microdynamics (hydration and dehydration) of such polymers means of Fourier transform infrared (FTIR) spectroscopy combined with two-dimensional analysis. Yushmanov et al.[27] performed T-jump NMR spectroscopy for PNIPAM and revealed that intermolecular aggregation (demixing) takes place faster than 1 s, being followed by a slow reorganization (<100 s). Villetti et al.[28] also found a slow relaxation component for a methylcellulose/salt aqueous solution by means of a small-angle light-scattering measurement. Furthermore, it should be particularly noted that Ye et al.[29] performed T-jump fluorescence spectroscopy to reveal two stages (two temporal regimes, 0.1 and 0.8 ms) in the coil-globule phase transition process.

Also, we recently developed a laser temperature-jump (T-jump) technique combined with time-resolved spectroscopy and spectrometry, and applied the technique to measure the dynamics of the coil-globule phase

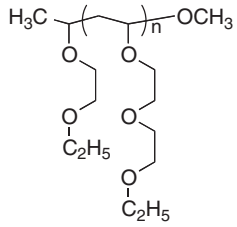

Figure 1. Chemical Structure of poly(EOEOVE).

transition[30] and the PS[31] of aqueous PNIPAM solutions. For fluorescence-labeled PNIPAM with $\overline{M}_w = 2 \times 10^4$, we determined the time constant of coil-globule phase transition to be $\tau = 35$ μs by monitoring the dynamic Stokes shift of a fluorescence probe whose emission wavelength maximum is sensitive to the dielectric environment surrounding the probe.[30] Furthermore, we also determined the time constant of PS (τ_{PS}) for PNIPAM by systematically varying $\overline{M}_w$ ($1 \times 10^5 \approx 1 \times 10^6$), and revealed that τ_{PS} is of the order of several tens of milliseconds (ms) and becomes larger (PS became slower) with increasing $\overline{M}_w$.[31] For gain further understanding of the PS mechanism, it is very important to obtain deeper insight into other factors governing PS dynamics, and the most worthwhile challenge would be to determine the chemical structures of sample polymers.

In the present study, we singled out poly[(2-ethoxy) ethoxy ethyl vinyl ether] (poly(EOEOVE)) as a target sample that is a member of an alternative major thermoresponsive polymer family, poly(alkyl vinyl ether). The chemical structure of poly(EOEOVE) is shown in Figure 1. One characteristic of the present polymer system is monodispersion in $\overline{M}_w$, which is achieved using living cationic polymerization.[32–34] By means of our technique, we focus our attention on the initial stage of the PS, corresponding to the temoral region (1 ms ≈ 1 s) just after the phase transition and before the slow reorganization process. Our technique is complementary with other relevant methodology described above. We successfully determined τ_{PS} with high accuracy for aqueous poly(EOEOVE) solutions by varying both $\overline{M}_w$ and concentration systematically. We demonstrated that the PS behavior of the polymer is quite sensitive to both of these factors ($\overline{M}_w$ and concentration) and is very different from the PS of PNIPAM systems. For instance, the PS of poly(EOEOVE) is much faster than that of PNIPAM. Based on these intriguing facts that have been obtained, we discuss the PS mechanism for the polymer, comparing it with PNIPAM systems.

2. Experimental Section

Milli-Q water was used as a solvent. Poly(EOEOVE) samples were synthesized by living cationic polymerization in a similar

Table 1. Fundamental properties of samples used here. $\overline{M}_w$, weight-average molecular weight; $\overline{M}_n$, number-average molecular weight; T_{ps}, lower critical solution temperature (LCST); R_H, hydrodynamic radius.

	$\overline{M}_w$	$\overline{M}_w/\overline{M}_n$	T_{ps} [°C]	R_H [nm]
PEO-68	6800	1.05	48.5	1.8
PEO-110	11 000	1.03	46.1	2.8
PEO-170	17 000	1.03	45.3	4.5
PEO-240	24 000	1.09	43.2	8.3
PEO-430	43 000	1.11	42.4	7.8

manner as used in our previous work.[32–34] The end group structure, shown in Figure 1, was determined using MALDI-TOF-MS. The characteristic feature of the synthesis is the supply of monodisperse polymers (with respect to molecular weight). For the sample polymers used here, the fundamental properties such as $\overline{M}_w$ (weight-average molecular weight), polydispersity $\overline{M}_w/\overline{M}_n$ (where $\overline{M}_n$ is the number-average molecular weight), the PS temperature (LCST; T_{ps}) of a 1.0 wt% aqueous solution, and the hydrodynamic radius (R_H) are summarized in Table 1. LCST was determined as a clouding point by a optical transmittance measurement. Here, for convenience, each sample is named on the basis of $\overline{M}_w$, ranging from 6800 ≈ 43 000. For instance, the polymer with $\overline{M}_w$ = 17 000 was termed as PEO-170. $\overline{M}_w$ and $\overline{M}_n$ were measured by means of gel permeation chromatography, while R_H was measured using a dynamic light-scattering (DLS) method (Otsuka Electronics, FDLS-3000).

The details of the nanosecond laser T-jump technique employed in the present study were already presented in our previous studies,[30,31] and are described here briefly. The fundamental output of a nanosecond-pulsed neodymium-doped yttrium aluminium garnet (Nd:YAG) laser (FWHM ≈ 10 ns, λ = 1064 nm) was focused onto a $Ba(NO3)_2$ crystal placed in an optical cavity to convert the wavelength to 1200 nm through a stimulated Raman effect. The 1200 nm, nanosecond light was used as a heating pulse, since water has a significant absorption at this wavelength due to an overtone of the O−H stretching mode. A quartz cell with optical path length = 1.0 mm was filled with an aqueous polymer solution, and maintained at a temperature that was marginally lower (≈1 K) than T_{ps} using a temperature controller. Then, the sample cell was irradiated with a single 1200 nm heating pulse to induce a T-jump. Simultaneously, a continuous-wave visible laser light (532 nm) was also introduced into the cell coaxially with the heating pulse, and the temporal change in the intensity of the transmitted light was measured with a fast photo-diode and a digital oscilloscope (500 MHz). In our study, the cloud point is defined as PS temperature (T_{ps}), although Kawaguchi et al.[35] pointed out that they do not equal top each other in a precise sense.

That is, the dynamic PS behavior was monitored and recorded as a time-dependent decay of transmitted light intensity due to an increase in turbidity resulting from the PS. The decrease in transmitted light intensity directly corresponds to an increase in scattered light intensity from the irradiated area of sample solutions. The increase in scattered light intensity should originate from two processes: one is an increase in the number of phase-separated microdomains, whereas the other one is an increase (growth) of the size of domains. Both processes are reflected to the observed light signals, and hardly separated at present. The time origin was defined as the time when the heating pulse reached the cell. The time constants of PS were determined by averaging the experimental results over 20 sets of measurements. It should be noted that the temperature rise (ΔT) upon the T-jump was suppressed to be $\Delta T < 2$ K (estimated using absorption coefficient and light intensity), because the present polymer system exhibited a sharp PS response with respect to changing temperature and large values for ΔT were frequently observed that affected the PS dynamics. To be more rigorous, the transmitted light intensity should be a function both of time and temperature. This situation could result in a complicated temporal behavior of the transmitted light intensity, since temperature also depends upon time. In the present study, time region of PS is of the order of milliseconds to several tens of milliseconds, while that of T-jump is nanosecond; much faster jump. In addition, cooling (which leads to re-mixing of a sample solution) takes place in much slower time region over several hundreds of milliseconds or seconds. Therefore, these processes can completely be separated on a time axis and hence the transmitted light intensity can be regarded as function of time. This situation holds also for PNIPAM systems as reported in our previous works.[30,31] Thus, the small ΔT was sufficient to observe the PS dynamics clearly.

3. Results and Discussion

3.1. Molecular Weight and Concentration Dependence of Hydrodynamic Radius

Prior to studying the PS dynamics, we systematically investigated R_H of the sample polymers as a function of $\overline{M}_w$ and concentration, because R_H directly reflects the structures of the polymers in aqueous solution and therefore could affect the PS dynamics. Figure 2a shows representative results of DLS measurements for dilute sample solutions (0.1 wt%), where mutual entanglements among the polymer chains are negligible. These were measured at room temperature, corresponding to homogeneous sample solutions (before PS). As can be obviously seen in the figure, all of the sample solutions exhibited two peaks in the DLS histograms; one is observed around R_H 0 to 10 nm, whereas the other one is observed over 100 nm. The smaller R_H distribution is clearly ascribable to individual single polymer chains (isolated from each other), whereas the larger R_H distribution would originate from polymer aggregates. Recently, Aoshima and co-workers[36,37] have also detected such poly(EOEOVE) aggregates in aqueous solution using DLS and size exclusion chromatography. Namely, polymer aggregation is also verified in the present work.

Figure 2b shows the concentration dependence of the DLS histogram for PEO-170 (poly(EOEOVE) with $\overline{M}_w$ = 17 000). Inspection of the results reveals one

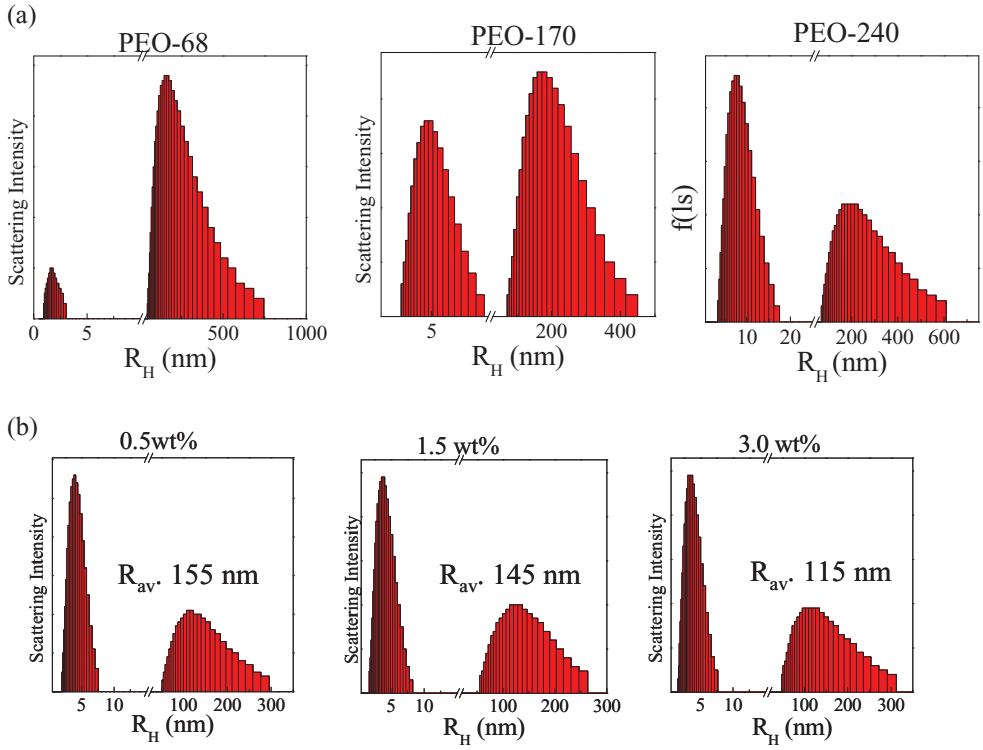

Figure 2. Representative results of DLS measurements. Sample names are given in the figure. The histograms were based on scattering intensity. (a) Molecular weight dependence. Solution concentration is 0.1 wt%. (b) Concentration dependence for PEO-170. Concentration of sample solution is given in the figure. R_H for aggregate in averaged value is also shown in the figure.

characteristic: the R_H values of single polymer chains hardly depend upon polymer concentration, whereas R_H of the aggregate material becomes lower with increasing concentration. Such behavior is consistent with the results in the previous work,[36,37] where the important role of the hydrophobicity of the side chains was pointed out in the aggregation.

3.2. Fundamental Characteristics of PS Dynamics

We systematically determined the PS time constants of the sample solutions using the T-jump technique, based on which we now discuss the PS mechanisms. Figure 3 shows representative temporal traces for transmittance [$T(t)$ in%] that reflect the PS dynamics at an early stage (PEO-240, 3.0 wt% solution) and a late stage (PEO-430, 3.0 wt%) in the process. In the early stage (several tens of milliseconds after the T-jump, Figure 3a), the value of $T(t)$ dropped precipitously from the initial value [$T(t)$ = 100%, corresponding to the homogeneous transparent solution] immediately after the T-jump. This corresponds to PS accompanying an increase in the turbidity of the sample solution. On the other hand, $T(t)$ gradually recovered to the initial value in the late stage (several seconds after the T-jump, Figure 3b), corresponding to phase-mixing due to cooling of the sample solution.

The analysis of $T(t)$ in the early stage provides the time constant of PS. For all of the sample solutions, (t) curves were successfully obtained with high signal/noise (S/N)

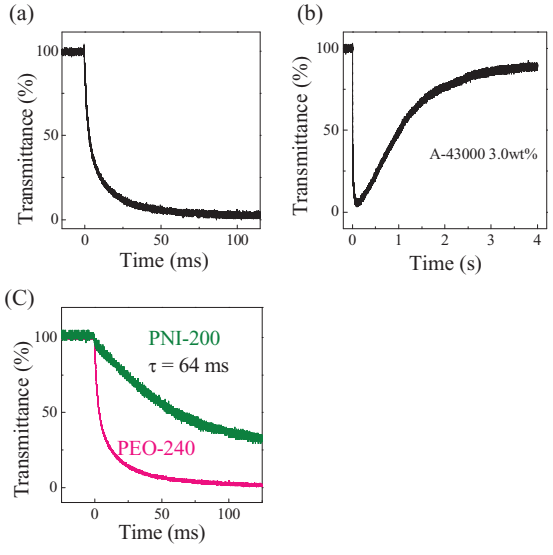

Figure 3. Representative results of transient transmittance T (t) measurements. Early stage after T-jump. Sample was PEO-240 solution (3.0 wt%). (a) Late stage after T-jump. Sample was PEO-430 solution (3.0 wt%). (b) Comparison of 3.0 wt% PEO-240 solution (purple line) and 3.0 wt% PNIPAM ($\overline{M}_w$ = 20 000) solution (green line).

ratios. They could never be reproduced with single-exponential functions, but instead fitted well with double exponential functions,

$$T(t) = A_1\exp(-t/\tau_1) + A_2\exp(-t/\tau_2) + B, \quad (1)$$

where τ_1 and τ_2 are the time constants of the fast and slow components in PS, respectively. A_1, A_2 correspond to pre-exponential factors, and B is a fitting constant. By fitting the value of $T(t)$ observed in the early stage (i.e., Figure 3a,c) with Equation (1), the PS time constants can be determined with high accuracy. The fast and slow components were revealed to fall within the ranges between $\tau_1 = 2 \approx 30$ ms and $\tau_2 = 20 \approx 120$ ms, respectively, which depended upon $\overline{M}_w$ and on the concentration (see later). It should be noted here that such PS behavior with double exponential functions is obviously different from the case of PNIPAM, where PS can be well described with single exponential functions: $T(t) = A\ \exp(-t/\tau_3) + B$, where τ_3 is a time constant of PS in an aqueous PNIPAM solution. Although the polydispersity of PNIPAM system ($\overline{M}_w/\overline{M}_n >$ 1.5) was larger than that of present poly(EOEOVE) system ($\overline{M}_w/\overline{M}_n \approx 1.0$), the PNIPAM system showed a single exponential behavior.[30] In this meaning, it is intriguing that the monodisperse poly(EOEOVE) system exhibits the biexponential behavior.

A comparison of poly(EOEOVE) with PNIPAM also revealed another emphatic difference. Figure 3c shows the $T(t)$ curve of a 3.0 wt% PEO-240 solution, together with the curve of a 3.0 wt% solution of PNIPAM with a similar $\overline{M}_w$ (= 20 000). Although the molecular weights were close to each other, the $T(t)$ curve of the PEO-240 solution exhibited a markedly faster decay than that of the PNIPAM solution. The PS time constant of the PEO-240 solution was determined to be $\tau_1 = 2.7$ ms, while τ was determined to be 64 ms for the PNIPAM solution. To be specific, the poly(EOEOVE) system can respond much more rapidly to temperature rises in PS than the PNIPAM system. The faster response is favorable from a viewpoint of the drug release application, and the origin of the behavior is discussed in a later section.

3.3. Concentration and Molecular Weight Dependence of PS Dynamics

For all of the poly(EOEOVE) samples examined here, we observed concentration (C) -dependent PS dynamics. Figure 4 displays representative results of $T(t)$ curves as a function of C (0.5 ≈ 5.0 wt%) for PEO-68, 170, and 240. As clearly shown in the figures, PS became faster with increasing C with high sensitivity. By analyzing these $T(t)$ curves we obtained further insights, including the C-dependences of τ_1, τ_2, and the ratio of each relative contribution (A_1 and A_2). In Figure 5, τ_1, τ_2, and $A_1/(A_1+A_2)$ are plotted against C for the 5 samples. We can clearly see that both the fast (τ_1) and slow (τ_2) PS processes became faster with increasing C. In the fast component (Figure 5a), PEO-110, 170, 240, 430 followed similar dependences, whereby

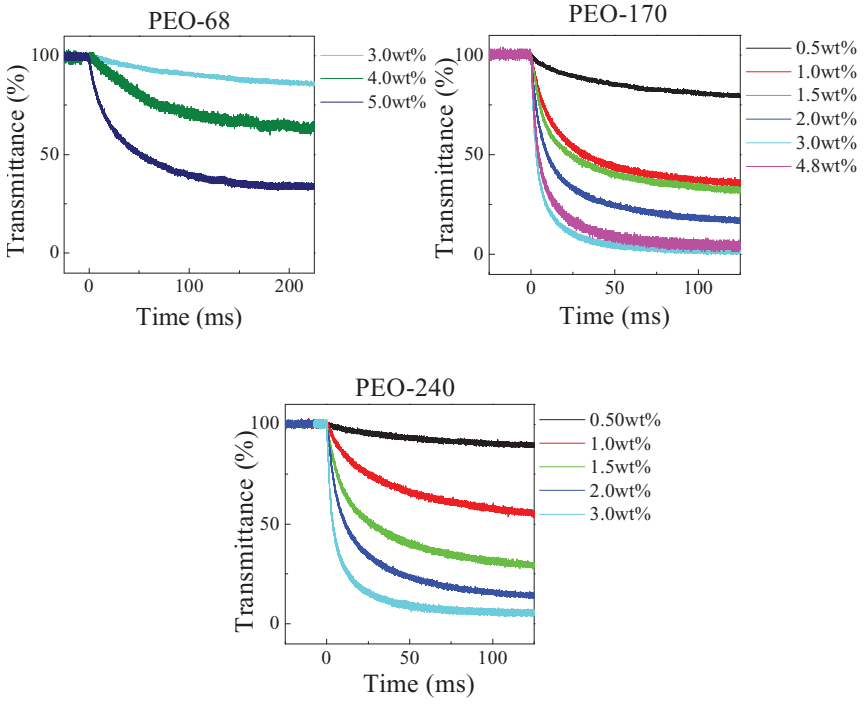

Figure 4. Concentration dependence of PS dynamics. Sample name and concentration is given in the figure.

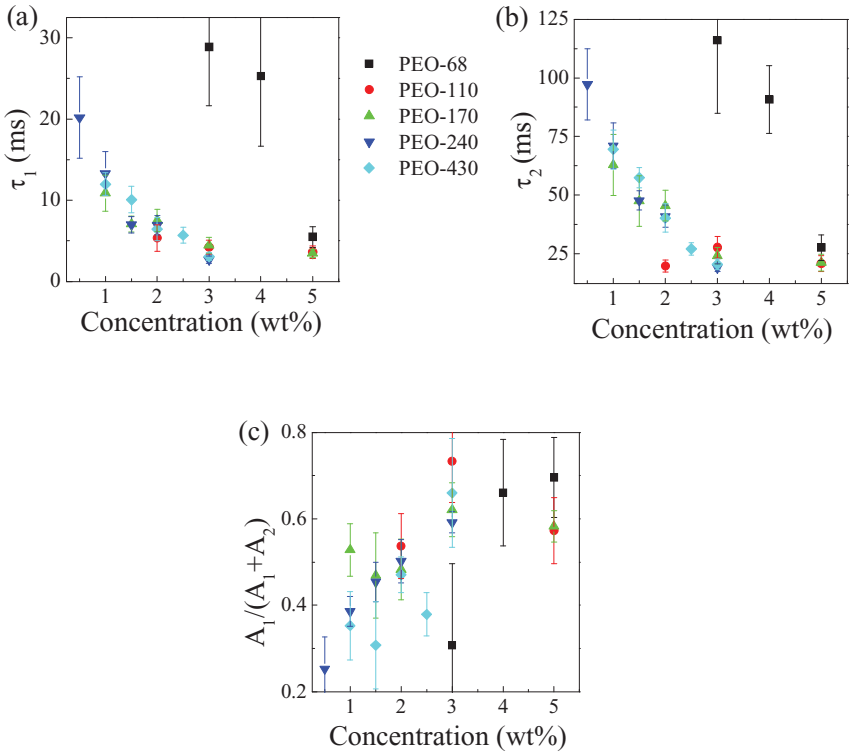

Figure 5. Concentration dependence of PS dynamics. (a) Fast component (τ_1). (b) Slow component (τ_2). (c) Relative contribution of the fast component ($A_1/(A_1+A_2)$).

τ_1 became smaller from 20 ms to 2 ms with increasing C from 1.0 to 5.0 wt%, while only PEO-68 deviated from the dependence and showed a slower PS response, varying from 30 to 5 ms. Qualitatively, the same behavior was also observed for the slow component τ_2 (Figure 5b). On the other hand, the relative contribution of the fast component ($A_1/(A_1+A_2)$) increased with increasing C, as shown in Figure 5c. Thus, we revealed that the C-dependent behavior, whereby the total PS process becomes faster with increasing C, has two meanings. First, both of the components became faster in denser solutions. Second, the fast component became dominant as C increased. These C-dependent effects are reflected the total C-dependent PS dynamics.

It should be noted that the PS dynamics were also sensitive to the $\overline{M}_w$ of the polymer. As expected from the results of Figure 5 and as shown in Figure 6, PS became faster with increasing $\overline{M}_w$. Upon changing $\overline{M}_w$ from 17 000 to 43 000, τ_1 and τ_2 decreased to about a half and a third of their original values, respectively. Again, the behavior observed for poly(EOEOVE) systems stands in contrast to the PNIPAM systems, where PS becomes slower with increasing $\overline{M}_w$. These experimental results should strongly reflect the PS mechanism, which is discussed in the following section.

3.4. PS Mechanism of Aqueous Poly(EOEOVE) Solutions

By integration of the experimental results described above, the PS characteristics of aqueous poly(EOEOVE) solutions can be summarized as follows:

(1) The PS dynamics consists of two processes, expressed by Equation (1).
(2) The faster and slower processes take place in the temporal ranges between $\tau_1 = 2 \approx 30$ ms and $\tau_2 = 20 \approx 120$ ms, respectively.
(3) With increasing C (concentration), both of the PS processes get faster, and the relative contribution of the faster process increases.
(4) The PS dynamics is slightly sensitive to $\overline{M}_w$.
(5) The behavior of (1), (2), and (4) are totally different from that of the PNIPAM system.

Based on these results, we discuss here a fundamental mechanism underlying the PS of aqueous poly(EOEOVE) solutions. As previously described, poly(EOEOVE) forms molecular aggregates whose averaged R_H values are several hundreds of nanometers. What is important here is that such aggregates have never been observed for aqueous PNIPAM solutions of $C < 5$ wt%. Accordingly, the origin of the two PS components that were peculiar to poly(EOEOVE) should be connected with the presence of

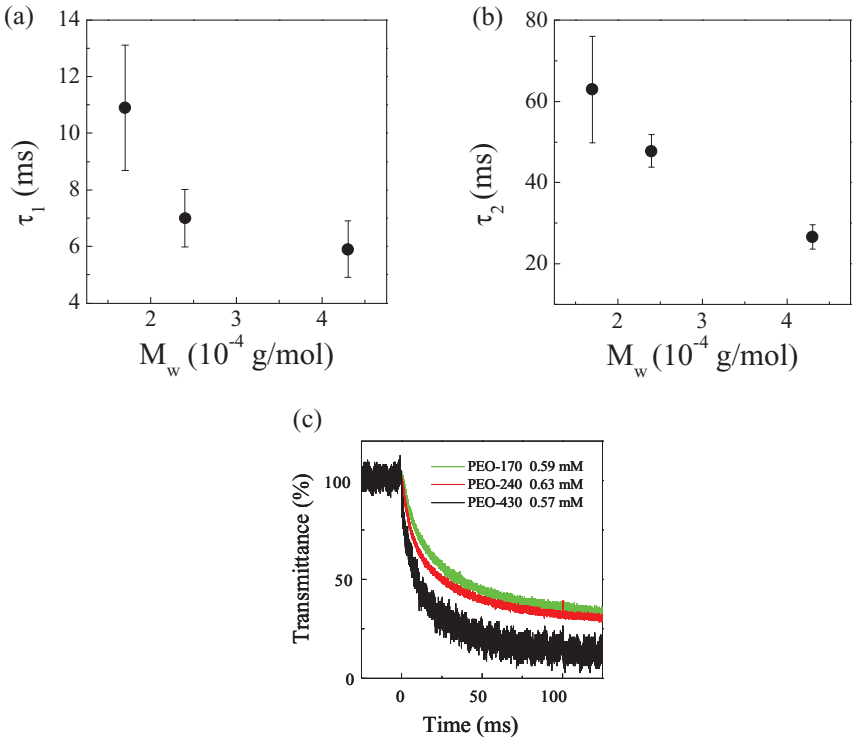

Figure 6. Molecular weight dependence of PS dynamics. Samples are PEO-170 (0.59 × 10^{-3} M), PEO-240 (0.63 × 10^{-3} M), and PEO-430 (0.57 × 10^{-3} M). (a) Fast component (τ_1). (b) Slow component (τ_2). (c) Representative traces of transient transmittance $T(t)$.

the aggregates. In the PS of PNIPAM solution, we detected only one component whose time constant (τ_3) was between 20 and 100 ms. These τ_3 values are close to the slower PS component (τ_2) in the poly(EOEOVE) systems, and the fast PS component (τ_1) was never observed for the PNIPAM system. Therefore, the origin of fast PS component should be ascribed to the aggregates. The formation of aggregates is presumably promoted with increasing C, and indeed, the relative contribution of the fast component [$A_1/(A_1+A_2)$] became larger as C increased (Figure 5c). It is generally accepted that the total PS process consists of two steps. First, the hydrated coils turn into globules accompanied by dehydration (phase transition). Second, the globules coalesce by diffusion and hydrophobic interactions, resulting in the formation of a polymer-rich phase and a water-rich phase (PS). When molecular aggregates are already formed before the temperature rise, the growth rate of the assembly is apparently large, resulting in the faster PS (τ_1) in poly(EOEOVE) solutions.

It should be noted again that τ_1 became smaller (PS became faster) with increasing C. This behavior is interpretable within the framework of aggregation. As previously described, and already reported,[36,37] the size (R_H) of the aggregates became smaller with increasing C. The smaller size would accordingly be maintained after the coil-globule phase transition. The smaller aggregates presumably diffuse faster in water, leading to the faster PS. Thus, the fast PS component (τ_1) should become faster still with increasing C, as clearly demonstrated in Figure 5a. It should be noted here that interchain aggregation even below LCST (meaning before PS) was also discussed for a block copolymer system of poly(EOEOVE) and octadecyl vinyl ether,[38] reinforcing our deduction where intermolecular aggregates play an important role in PS.

On the other hand, based on the above discussion, the origin of the slow PS component (τ_2) should be related to poly(EOEOVE) molecules escaping from the aggregation. Each individual polymer chain would undergo the normal PS process. With increasing C, the averaged intermolecular distance (which corresponds to the interglobular distance) becomes smaller. The closer intermolecular distance (interpolymer chain center-to-center distance) leads to faster PS, as verified in Figure 5b. Furthermore, Sato and co-workers[36] investigated concentration dependence of T_{ps} (LCST) for a poly(EOEOVE) system. In a low concentration regime (C < 10 wt%), T_{ps} decreased with increasing C, implying that hydrophobic (or some attractive) interactions among polymer chains are enhanced with increasing C. This effect would also contribute to the observed C-dependent τ_1 and τ_2.

Finally, we will now briefly discuss the dependence of PS on the $\overline{M}_w$. In the previous study, we revealed that

the PS of the PNIPAM system ($\overline{M}_w = 1 \times 10^5 \approx 1 \times 10^6$) became appreciably slower with increasing $\overline{M}_w$. This is the opposite to the observation in the present case, where PS became somewhat faster with increasing $\overline{M}_w$. In the present case, the $\overline{M}_w$ of the material that was examined is much lower than that in the PNIPAM systems. In the present poly(EOEOVE) system, LCST (T_{ps}) was observed to decrease with increasing $\overline{M}_w$ (Table 1). This means that the hydrophobic property would be enhanced with increasing $\overline{M}_w$. Accordingly, hydrophobic interactions would be enhanced with increasing $\overline{M}_w$, resulting in faster PS.

4. Conlusion

In the present study, we have systematically revealed the PS dynamics of aqueous poly(EOEOVE) solutions by means of a laser T-jump technique. The outcome was totally different from that for a PNIPAM system. Both fast and slow PS processes were detected, and both of these processes were very sensitive to *C*, and also depended somewhat upon $\overline{M}_w$. One of the important findings here is that the PS of poly(EOEOVE) is much faster than that of PNIPAM in aqueous solutions, and PS became even faster with increasing *C*. This PS behavior, which is peculiar to the present system, was successfully understood within the framework of the aggregation mechanism. Namely, it has been demonstrated that the PS dynamics reflect the initial condition of the polymer structure in the solution. This important information will provide a useful guide to designing novel stimuli-responsive polymers with the desired PS responses.

Acknowledgements: This work was partly supported by a Grant-in-Aid for Scientific Research from the Ministry of Education, Culture, Sports, Science and Technology of Japan to the Priority Area "Strong Photon-Molecule Coupling Fields (470)" (No. 19049004), No. 20550002, and the Global COE Program (Project No. B01: Catalysis as the Basis for Innovation in Materials Science). T.S. was supported as a Research Fellow of the Japan Society for the Promotion of Science (JSPS Research Fellow).

Received: September 28, 2011; Revised: November 8, 2011; Published online: December 13, 2011; DOI: 10.1002/macp.201100540

Keywords: hydrogels; kinetics; phase separation; stimuli-sensitive polymers

[1] H. Heskins, J. E. Guillet, *J. Macromol. Sci., Chem.* **1968**, *A2*, 1441.
[2] S. T. Sun, I. Nishino, G. Swislow, T. Tanaka, *J. Chem. Phys.* **1980**, *73*, 5971.
[3] F. M. Winnik, *Macromolecules* **1990**, *23*, 233.
[4] R. Koningsveld, W. H. Stockmayer, E. Nies, *Polymer Phase Diagrams*, Oxford University Press, New York **2001**.
[5] D. Schmaljohann, *Adv. Drug Delivery Rev.* **2006**, *58*, 1655.
[6] F. Segui, X.-P. Qiu, F. M. Winnik, *Polymer* **2008**, *46*, 314.
[7] K. Kubota, S. Fujishige, I. Ando, *J. Phys. Chem.* **1990**, *94*, 5154.
[8] F. M. Winnik, *Macromolecules* **1990**, *23*, 233.
[9] Y. Maeda, H. Yamauchi, T. Kubota, *Langumir* **2009**, *25*, 479.
[10] Y. Satokawa, T. Shikata, F. Tanaka, X.-P. Qiu, F. M. Winnik, *Macromolecules* **2009**, *42*, 1400.
[11] Y. Katsumoto, N. Kubosaki, *Macromolecules* **2008**, *41*, 5955.
[12] T. Mori, T. Hirano, A. Maruyama, Y. Katayama, T. Niidome, Y. Bando, K. Ute, S. Takaku, Y. Maeda, *Langmuir* **2009**, *25*, 48.
[13] N. Osaka, S. Miyazaki, S. Okabe, H. Endo, A. Sasai, K. Seno, S. Aoshima, M. Shibayama, *J. Chem. Phys.* **2007**, *127*, 094905.
[14] H. G. Schild, D. A. Tirrell, *J. Phys. Chem.* **1990**, *94*, 4352.
[15] J. Zhao, R. Hoogenboom, G. V. Assche, B. Van Mele, *Macromolecules* **2010**, *43*, 6853.
[16] X. Zhou, J. Li, J. C. Wu, B. Zheng, *Macromol. Rapid Commun.* **2008**, *29*, 1363.
[17] T. Tanaka, D. J. Fillmore, *J. Chem. Phys.* **1979**, *70*, 1214.
[18] T. Tanaka, E. Sato, Y. Hirokawa, S. Hirotsu, J. Peetermans, *Phys. Rev. Lett.* **1985**, *55*, 2455.
[19] E. Sato Matsuo, T. Tanaka, *J. Chem. Phys.* **1988**, *89*, 1695.
[20] M. Shibayama, *Macromolecular Chem. Phys.* **1998**, *199*, 1.
[21] K. Van Durme, G. Van Assche, B. Van Mele, *Macromolecules* **2004**, *37*, 9596.
[22] K. Van Durme, S. Verbrugghe, F. E. Du Prez, B. Van Mele, *Macromolecules* **2004**, *37*, 1054.
[23] S. Swier, K. Van Durme, B. Van Mele, *J. Polym. Sci., Part B: Poym. Phys.* **2003**, *41*, 1824.
[24] J. Zhao, J. Shan, G. Van Assche, H. Tenhu, B. Van Mele, *Macromolecules* **2009**, *42*, 5317.
[25] B. Sun, Y. Lin, P. Wu, H. W. Siesler, *Macromolecules* **2008**, *41*, 1512.
[26] B. Sun, H. Lai, P. Wu, *J. Phys. Chem. B* **2011**, *115*, 1335.
[27] P. Yushmanov, I. Furo, I. Iliopoulos, *Macromol. Chem. Phys.* **2006**, *207*, 1972.
[28] M. A. Villetti, V. Soldi, V. C. Rochas, R. Borsali, *Macromol. Chem. Phys.* **2011**, *212*, 1063.
[29] X. Ye, Y. Lu, L. Shen, Y. Ding, S. Liu, G. Zhang, C. Wu, *Macromolecules* **2007**, *40*, 4750.
[30] Y. Tsuboi, Y. Yoshida, N. Kitamura, K. Iwai, *Chem. Phys. Lett.* **2009**, *468*, 42.
[31] Y. Tsuboi, Y. Yoshida, K. Okada, N. Kitamura, *J. Phys. Chem. B* **2008**, *112*, 2562.
[32] S. Aoshima, H. Oda, E. Kobayashi, *J. Polym. Sci., Part A: Polym. Chem.* **1992**, *30*, 2407.
[33] S. Aoshima, S. Sugihara, M. Shibayama, S. Kanaoka, *Macromol. Symp.* **2004**, *215*, 151.
[34] S. Aoshima, S. Kanaoka, *Chem. Rev.* **2009**, *109*, 5245.
[35] T. Kawaguchi, K. Kobayashi, K. Osa, T. Yoshizaki, *J. Phys. Chem. B* **2009**, *113*, 5440.
[36] H. Matsuda, Y. Miyazaki, S. Sugihara, S. Aoshima, K. Saito, T. Sato, *J. Polym. Sci., Part B: Polym. Phys.* **2005**, *43*, 2937.
[37] Y. Matsuda, T. Kawata, S. Sugihara, S. Aoshima, T. Sato, *J. Polym. Sci., Part B: Polym. Phys.* **2006**, *44*, 1189.
[38] K. Kono, T. Murakami, T. Yoshida, Y. Haba, S. Kanaoka, T. Takagishi, S. Aoshima, *Bioconjugate Chem.* **2005**, *16*, 1367.